Available online at www.sciencedirect.com
ScienceDirect
Nuclear Physics B Proceedings Supplement 00 (2014) 1–6
Nuclear Physics B Proceedings Supplement

Higgs Physics at CLIC

Eva Sicking on behalf of the CLICdp collaboration

CERN, 1211 Geneva 23, Switzerland

Abstract

The Compact Linear Collider (CLIC) is an attractive option for a future multi-TeV linear electron-positron collider, offering the potential for a rich precision physics programme, combined with sensitivity to a wide range of new phenomena. The physics reach of CLIC has been studied in the context of three distinct centre-of-mass energies, $\sqrt{s}$ = 350 GeV, 1.4 TeV and 3.0 TeV. This staged scenario provides an excellent environment for precise studies of the properties of the 126 GeV Higgs boson. Operation at $\sqrt{s}$ = 350 GeV allows, on the one hand, for a determination of the couplings and width of the Higgs boson in a model-independent manner through the study of the Higgsstrahlung process, and on the other hand, for a study of Higgs bosons produced in W^+W^- fusion for the most common Higgs decay modes. Operation at higher centre-of-mass energies, $\sqrt{s}$ = 1.4 TeV and 3 TeV, provides high statistics W^+W^- fusion samples allowing for high precision measurements of many Higgs couplings and a study of rare Higgs decay modes, Higgs boson samples produced in ZZ fusion, and the potential to study the top Yukawa coupling as well as the Higgs boson self-coupling. We explore the potential of the CLIC Higgs physics programme based on full simulation studies of a wide range of final states. The evolution of the physics sensitivity as a function of the centre-of-mass energy is presented in terms of combined fits to all measurements and their respective statistical uncertainty.

Keywords: Physics potential, Higgs, Compact Linear Collider

1. Introduction

The Compact Linear Collider (CLIC) is a mature option for a future multi-TeV e^+e^- collider. It is based on a two-beam acceleration scheme using normal-conducting cavities which achieve gradients of 100 MV/m [1]. CLIC is planned to be built in a staged construction with three centre-of-mass (cms) energies ranging from few hundred GeV to 3 TeV with energies adapted to known processes and future discoveries at the LHC. The currently studied scenario foresees 4–5 years of operation per energy stage with luminosities of the order of $10^{34}\,\mathrm{cm}^{-2}\mathrm{s}^{-1}$, resulting in an integrated luminosity of 500 fb^{-1} at $\sqrt{s}$ = 350 GeV, 1.5 ab^{-1} $\sqrt{s}$ = 1.4 TeV, and 2 ab^{-1} at $\sqrt{s}$ = 3 TeV allowing for a rich Higgs physics programme [2, 3].

Email address: eva.sicking@cern.ch (Eva Sicking on behalf of the CLICdp collaboration)

Table 1: Number of Higgs events expected for the studied CLIC staging scenario and for the most relevant production processes. The numbers are estimated for a Higgs mass of m_H = 125 GeV using initial state radiation, the CLIC beam spectrum, and unpolarised beams. For −80% electron beam polarisation considered for CLIC, the listed numbers increase by 12% for ZH events and He^+e^- events, and by 80% for $H\nu_e\bar{\nu}_e$ events.

	350 GeV 500 fb^{-1}	1.4 TeV 1.5 ab^{-1}	3 TeV 2 ab^{-1}
# ZH events	68 000	20 000	11 000
# $H\nu_e\bar{\nu}_e$ events	17 000	370 000	830 000
# He^+e^- events	3 700	37 000	84 000
# $t\bar{t}H$ events	—	2 400	1 400
# $HH\nu_e\bar{\nu}_e$ events	—	225	1 200

Table 1 lists the number of Higgs events of the most relevant production processes expected in the studied CLIC staging scenario.

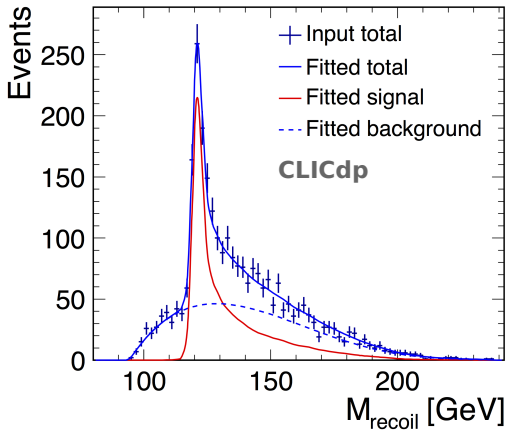

Figure 1: Recoil mass distribution for simulated $e^+e^- \to HZ \to H\mu^+\mu^-$ events with $m_H = 125\,\text{GeV}$ and all relevant background events after a pre-selection and a selection based on a multivariate analysis; measured with the CLIC_ILD detector concept at $\sqrt{s} = 350\,\text{GeV}$ using an integrated luminosity of $500\,\text{fb}^{-1}$ [4].

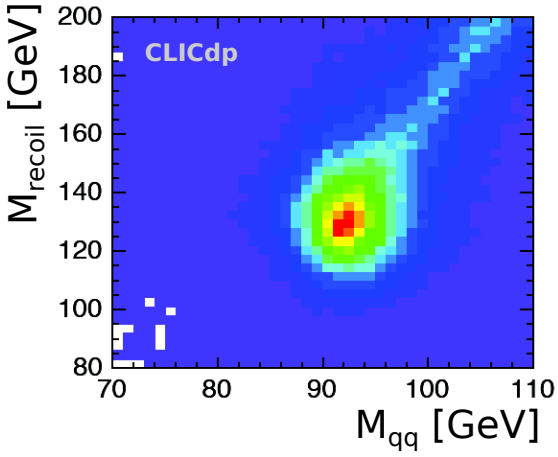

Figure 2: Correlation between the Z recoil mass and the reconstructed Z mass for simulated $e^+e^- \to HZ \to H\,q\bar{q}$ events with $m_H = 126\,\text{GeV}$ for visible H decays after a pre-selection; measured with the CLIC_ILD detector concept at $\sqrt{s} = 350\,\text{GeV}$ using an integrated luminosity of $500\,\text{fb}^{-1}$ [11].

2. Higgs benchmark studies

In order to estimate the physics potential of CLIC in terms of Higgs precision measurements, a comprehensive list of Higgs physics benchmark studies is currently being carried out [5]. The benchmark studies are based on full Geant4 [6, 7] detector simulations using the detector concepts CLIC_SiD and CLIC_ILD [2, 3] which are based on the detector concepts of the International Linear Collider [8]. In all studies, the software chain described in the CLIC Conceptual Design Report [2] is used. The detector simulations include pile-up from $\gamma\gamma \to$ hadron backgrounds as well as all relevant Standard Model (SM) background processes from e^+e^-, $e^\pm\gamma$ and $\gamma\gamma$ collisions taking into account the CLIC beam spectrum and initial state radiation.

The analysis results are presented in terms of achievable statistical precisions of various Higgs observables. At this stage, a detailed study of potential systematic uncertainties has not been performed, but based on the experience at past e^+e^- colliders, for example the Large Electron Positron collider (LEP), we believe that the statistical uncertainties will dominate the experimental systematic uncertainties.

For those studies which were completed before and shortly after the Higgs discovery at the LHC in 2012 [9, 10], a Higgs mass of $m_H = 120\,\text{GeV}$ and $125\,\text{GeV}$ has been used, recent analyses use $m_H = 126\,\text{GeV}$. It is expected that this variation of the Higgs mass between the different studies has only a minor impact on the analysis results in terms of the achievable precisions.

2.1. Higgsstrahlung

The measurement of events from the Higgsstrahlung process $e^+e^- \to ZH$ – the dominant Higgs production process at cms energies below $\sqrt{s} = 500\,\text{GeV}$ – allows for a precise measurement of, on the one hand, the coupling of the Higgs boson to the Z, and on the other hand, the couplings between the Higgs boson and its final states. A model-independent measurement of the coupling g_{HZZ} is performed with the reconstruction of the Z recoil mass

$$m^2_{recoil} = s + m^2_Z - 2E_Z \cdot \sqrt{s} \qquad (1)$$

with no reconstruction of the Higgs necessary. Thus it is possible to also study invisible Higgs decay modes. The Z recoil mass of events from the Higgsstrahlung process and all relevant backgrounds at $\sqrt{s} = 350\,\text{GeV}$ is shown in figure 1 for the Z decay to muons. Due to the clean reconstruction of the leptonic Z decay, a fully model independent measurement can be performed. From simulation studies of the Higgsstrahlung process at CLIC at $\sqrt{s} = 350\,\text{GeV}$ using only the $Z \to \mu^+\mu^-$ and $Z \to e^+e^-$ decay modes, an achievable precision on the cross section times branching ratio of $\Delta\sigma_{HZ}/\sigma_{HZ} \approx 4.2\%$ is estimated, which results in a precision on the coupling of $\Delta(g_{HZZ})/g_{HZZ} \approx 2.1\%$ [4].

A higher precision is achieved in simulation studies of the Higgsstrahlung process analysing the dominant hadronic Z decay mode with a branching ratio (BR) of 70% [11]. Even though the hadronic Z reconstruction depends slightly on the Higgs decay mode, a careful

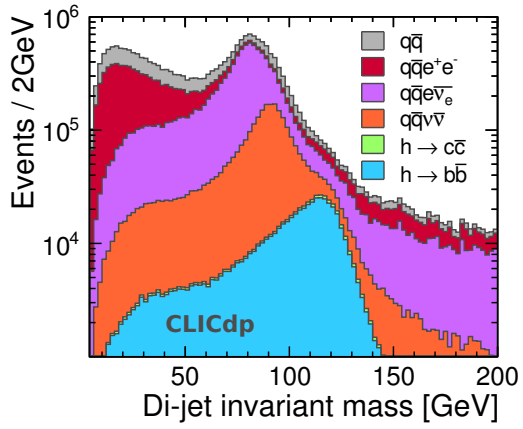

Figure 3: Di-jet invariant mass distribution for simulated $H \to b\bar{b}$ and $H \to c\bar{c}$ events with $m_H = 120\,\text{GeV}$ from the W^+W^- fusion process and events from all relevant background processes after a pre-selection; measured with the CLIC_SiD detector at $\sqrt{s} = 3\,\text{TeV}$ using an integrated luminosity of $2\,\text{ab}^{-1}$[2, 12].

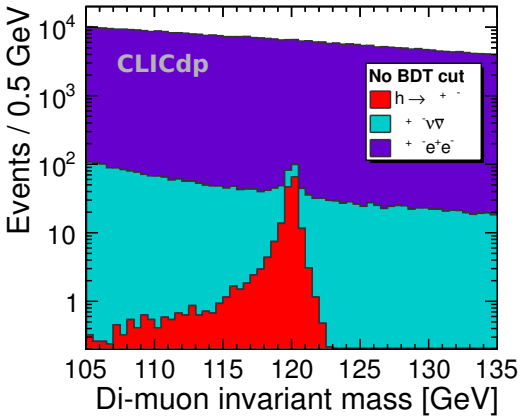

Figure 4: Invariant mass distribution of the di-muon system for simulated $H \to \mu^+\mu^-$ events with $m_H = 120\,\text{GeV}$ from the W^+W^- fusion process and events from the two main background processes after a pre-selection; measured with the CLIC_SiD detector at $\sqrt{s} = 3\,\text{TeV}$ using an integrated luminosity of $2\,\text{ab}^{-1}$[12, 14].

choice of the analysis variables makes the selection efficiencies almost model independent. As an example, the correlation of the Z recoil mass and the Z mass from the hadronic Z decay is shown in figure 2 for visible Higgs decays only. For the hadronic Z decay mode, the uncertainty of the coupling is estimated to have a precision of $\Delta\sigma_{HZ}/\sigma_{HZ} \approx 1.8\%$ resulting in $\Delta(g_{HZZ})/g_{HZZ} \approx 0.9\%$. In addition, selected final states of the Higgs decay are studied directly for the Higgsstrahlung process at $\sqrt{s} = 350\,\text{GeV}$. Table 2 summarises the precisions of the cross section times branching ratio for theses channels.

2.2. W^+W^- fusion

While the W^+W^- fusion process $e^+e^- \to H\nu_e\bar{\nu}_e$ already contributes a significant number of Higgs bosons at a cms energy as low as $\sqrt{s} = 350\,\text{GeV}$, above $\sqrt{s} = 500\,\text{GeV}$ it represents the production process with the largest cross section. Due to the large number of events, W^+W^- fusion allows for the study of the couplings in the most common Higgs decay modes at the percent level for the CLIC energy stages at $\sqrt{s} = 1.4\,\text{TeV}$ and 3 TeV. In addition, rare Higgs decay channels can be accessed.

As an example for a high precision Higgs measurement using the W^+W^- fusion process, figure 3 shows the di-jet invariant mass distribution for the Higgs decays $H \to b\bar{b}$ (BR = 56%) and $H \to c\bar{c}$ (BR = 3%), together with all relevant SM backgrounds. Based on the flavour tagging capabilities of the CLIC detector concepts and the clean environments in e^+e^- collisions, an efficient separation of the different hadronic final states of the Higgs decay can be performed resulting in statistical uncertainties of $\Delta(\sigma(H\nu_e\bar{\nu}_e) \times \text{BR}(H \to b\bar{b})) = 0.2\%$ and $\Delta(\sigma(H\nu_e\bar{\nu}_e) \times BR(H \to c\bar{c})) = 2.7\%$ [2, 12].

Figures 4 and 5 show examples of the study of two rare Higgs decays, $H \to \mu^+\mu^-$ with a branching ratio of 0.022% and $H \to Z\gamma$ with a branching ratio of 0.16%. Simulation studies of the $H \to \mu^+\mu^-$ channel achieve a precision on the cross section times branching ratio of 38% at $\sqrt{s} = 1.4\,\text{TeV}$ [13] and 16% at 3 TeV [12, 14]. Simulation studies of the $H \to Z\gamma$ decay channel including the hadronic Z decay as well as the Z decays to electrons and muons reach a combined precision of the cross section times branching ratio of 42% at $\sqrt{s} = 1.4\,\text{TeV}$ [15].

2.3. ZZ fusion

The ZZ fusion process $e^+e^- \to He^+e^-$ is the sub-leading Higgs production process at $\sqrt{s} = 1.4$ and 3 TeV, with a cross section around 10 times smaller than the one of the W^+W^- fusion process. For $\sqrt{s} = 1.4\,\text{TeV}$, events from the ZZ fusion process are currently studied in the most common decay mode $H \to b\bar{b}$ [16]. The precision of the cross section times branching ratio measurement is expected to be 1% at the cms energy of $\sqrt{s} = 1.4\,\text{TeV}$ and 0.7% at 3 TeV. A comparison between the $H \to b\bar{b}$ events produced in the ZZ fusion and in the W^+W^- fusion process will allow for a precise estimation of the ratio of the H-to-W and H-to-Z couplings, in which most

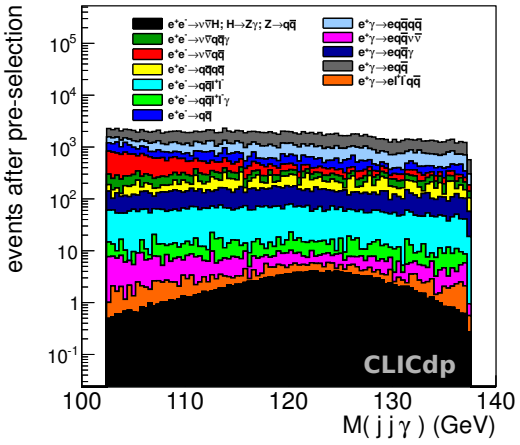

Figure 5: Invariant mass distribution of the di-jet and photon system for simulated $H \to Z\gamma; Z \to q\bar{q}$ events with $m_H = 126\,\text{GeV}$ from the W^+W^- fusion process and events from all relevant background processes after a pre-selection; measured with the CLIC_SiD detector at of $\sqrt{s} = 1.4\,\text{TeV}$ using an integrated luminosity of $1.5\,\text{ab}^{-1}$[15].

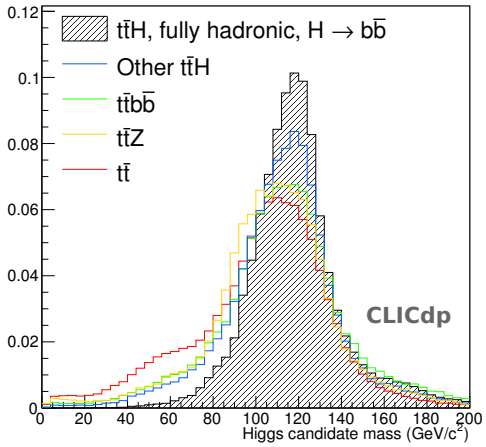

Figure 6: Invariant mass distribution of reconstructed Higgs candidates for simulated $t\bar{t}H$ events in the fully hadronic channel in comparison to events from all relevant $t\bar{t}$(+X)-based background processes without additional selection; measured with the CLIC_SiD detector at $\sqrt{s} = 1.4\,\text{TeV}$ using an integrated luminosity of $1.5\,\text{ab}^{-1}$[17]. All histograms are normalised to unity.

systematic uncertainties cancel out.

2.4. Top Yukawa coupling

The cms energy stage of $\sqrt{s} = 1.4\,\text{TeV}$ allows for the study of the $e^+e^- \to t\bar{t}H$ process, giving sensitivity to the top Yukawa coupling. Events with the most common $H \to b\bar{b}$ decay and two $t\bar{t}$ decay modes – the semi-leptonic and fully hadronic modes – are analysed [17]. This complex final state, with 6 to 8 jets including four b-jets, is an excellent detector benchmark process, testing jet reconstruction, flavour tagging, lepton identification, and reconstruction of missing energy. As an example, figure 6 shows the invariant mass distribution of the H candidate in the fully hadronic channel for signal events and events of the most relevant $t\bar{t}$(+X)-based background channels. The combined precision using these backgrounds is $\Delta\sigma(t\bar{t}H)/\sigma(t\bar{t}H) = 8.1\%$ resulting in a precision on the top Yukawa coupling of 4.3%. The impact of backgrounds not based on $t\bar{t}$ are under investigation, and are expected to have an effect at the few-per-mill level.

2.5. Higgs self-coupling

The process $e^+e^- \to HH\nu_e\bar{\nu}_e$ with sufficient cross sections at the cms energies of $\sqrt{s} = 1.4\,\text{TeV}$ and 3 TeV gives access to the Higgs trilinear self-coupling λ and the quartic coupling g_{HHWW} at the HHWW vertex.
One possibility to estimate the uncertainty of λ is to measure the $e^+e^- \to HH\nu_e\bar{\nu}_e$ cross section and converte its uncertainty to an uncertainty of the trilinear self-coupling with a conversion factor of 1.20 at $\sqrt{s} = 1.4\,\text{TeV}$ and 1.54 at 3 TeV. A second possibility is to perform a template fit of the neural net classifier response distribution which gives a direct estimation of the uncertainty of λ.
Simulation studies using the most common Higgs decay mode $HH \to b\bar{b}b\bar{b}$ as signal achieve a precision on the Higgs trilinear self-coupling of 32% at $\sqrt{s} = 1.4\,\text{TeV}$ and 16% at 3 TeV [5]. For −80% electron beam polarisation, this precision further improves to 24% and 12%. Preliminary studies of the quartic coupling g_{HHWW} result in an uncertainty of 7% at $\sqrt{s} = 1.4\,\text{TeV}$ and 3% at 3 TeV [5]. In the future, these results could be improved by adding analyses for other Higgs decay channels such as $HH \to b\bar{b}WW^*$. The analysis of these channels represents a challenge for the forward jet reconstruction.

3. Global fits

As indicated in the third column of table 2, the measured values of the cross section times branching ratio depend on the couplings g as well as on the total Higgs width Γ_H. To extract the values of the couplings and the Higgs width, a combined fit of each independent measurement and its respective statistical uncertainty listed in table 2

Table 2: Precisions obtainable for the Higgs observables at CLIC in the studied staging scenario [5, 18]. The numbers are estimated without beam polarisation. Numbers marked as * are preliminary and numbers marked as † are estimates. The table is a snapshot of the state of all analyses performed in the CLIC Higgs analysis working group from July 2014.

Channel	Measurement	Observable	Statistical precision		
			350 GeV 500 fb^{-1}	1.4 TeV 1.5 ab^{-1}	3.0 TeV 2.0 ab^{-1}
HZ	Recoil mass dist.	m_H	120 MeV	–	–
HZ	$\sigma_{HZ} \times BR_{H\to invisible}$	Γ_{inv}	0.6%	–	–
HZ	$H \to b\bar{b}$ mass dist.	m_H	tbd	–	–
$H\nu_e\bar{\nu}_e$	$H \to b\bar{b}$ mass dist.	m_H	–	40 MeV*	33 MeV*
HZ	$\sigma_{HZ} \times BR_{Z\to l^+l^-}$	g^2_{HZZ}	4.2%	–	–
HZ	$\sigma_{HZ} \times BR_{Z\to q\bar{q}}$	g^2_{HZZ}	1.8%	–	–
HZ	$\sigma_{HZ} \times BR_{H\to b\bar{b}}$	$g^2_{HZZ}g^2_{Hbb}/\Gamma_H$	1%†	–	–
HZ	$\sigma_{HZ} \times BR_{H\to c\bar{c}}$	$g^2_{HZZ}g^2_{Hcc}/\Gamma_H$	5%†	–	–
HZ	$\sigma_{HZ} \times BR_{H\to gg}$		6%†	–	–
HZ	$\sigma_{HZ} \times BR_{H\to\tau^+\tau^-}$	$g^2_{HZZ}g^2_{H\tau\tau}/\Gamma_H$	5.7%	–	–
HZ	$\sigma_{HZ} \times BR_{H\to WW^*}$	$g^2_{HZZ}g^2_{HWW}/\Gamma_H$	2%†	–	–
HZ	$\sigma_{HZ} \times BR_{H\to ZZ^*}$	$g^2_{HZZ}g^2_{HZZ}/\Gamma_H$	tbd	–	–
$H\nu_e\bar{\nu}_e$	$\sigma_{H\nu_e\bar{\nu}_e} \times BR_{H\to b\bar{b}}$	$g^2_{HWW}g^2_{Hbb}/\Gamma_H$	3%†	0.3%	0.2%
$H\nu_e\bar{\nu}_e$	$\sigma_{H\nu_e\bar{\nu}_e} \times BR_{H\to c\bar{c}}$	$g^2_{HWW}g^2_{Hcc}/\Gamma_H$	–	2.9%	2.7%
$H\nu_e\bar{\nu}_e$	$\sigma_{H\nu_e\bar{\nu}_e} \times BR_{H\to gg}$		–	1.8%	1.8%
$H\nu_e\bar{\nu}_e$	$\sigma_{H\nu_e\bar{\nu}_e} \times BR_{H\to\tau^+\tau^-}$	$g^2_{HWW}g^2_{H\tau\tau}/\Gamma_H$	–	3.7%*	tbd
$H\nu_e\bar{\nu}_e$	$\sigma_{H\nu_e\bar{\nu}_e} \times BR_{H\to\mu^+\mu^-}$	$g^2_{HWW}g^2_{H\mu\mu}/\Gamma_H$	–	38%	16%
$H\nu_e\bar{\nu}_e$	$\sigma_{H\nu_e\bar{\nu}_e} \times BR_{H\to\gamma\gamma}$		–	15%	tbd
$H\nu_e\bar{\nu}_e$	$\sigma_{H\nu_e\bar{\nu}_e} \times BR_{H\to Z\gamma}$		–	42%	tbd
$H\nu_e\bar{\nu}_e$	$\sigma_{H\nu_e\bar{\nu}_e} \times BR_{H\to WW^*}$	g^4_{HWW}/Γ_H	tbd	1.1%*	0.8%*
$H\nu_e\bar{\nu}_e$	$\sigma_{H\nu_e\bar{\nu}_e} \times BR_{H\to ZZ^*}$	$g^2_{HWW}g^2_{HZZ}/\Gamma_H$	–	3%†	2%†
He^+e^-	$\sigma_{He^+e^-} \times BR_{H\to b\bar{b}}$	$g^2_{HZZ}g^2_{Hbb}/\Gamma_H$	–	1%†	0.7%†
$t\bar{t}H$	$\sigma_{t\bar{t}H} \times BR_{H\to b\bar{b}}$	$g^2_{Htt}g^2_{Hbb}/\Gamma_H$	–	8%	tbd
$HH\nu_e\bar{\nu}_e$	$\sigma(HH\nu_e\bar{\nu}_e)$	g_{HHWW}	–	7%*	3%*
$HH\nu_e\bar{\nu}_e$	$\sigma(HH\nu_e\bar{\nu}_e)$	λ	–	32%	16%
$HH\nu_e\bar{\nu}_e$	with -80% e^- pol.	λ	–	24%	12%

is used based on a minimisation of

$$\chi^2 = \sum_i \frac{(\frac{C_i}{C_{i,\mathrm{SM}}} - 1)^2}{\Delta F_i^2}. \quad (2)$$

Here, C_i is the combination of Higgs couplings and total width, if applicable, for example, $C_{ZH} = g^2_{HZZ}$ and $C_{ZH,H\to b\bar{b}} = (g^2_{HZZ} \cdot g^2_{Hbb})/\Gamma_H$, and ΔF_i is the statistical uncertainty of the measurement, for example, $\Delta F_{ZH} = \delta(\sigma_{e^+e^-\to ZH})$ and $\Delta F_{ZH,H\to b\bar{b}} = \delta(\sigma_{e^+e^-\to ZH} \times BR_{H\to b\bar{b}})$. The fit procedure assumes that for all observables the SM expectation of the value is measured.

The resulting precisions of the Higgs observables are listed in table 3. They are obtained in a fully model independent approach, which is unique for lepton colliders and stems from the model independent ZH measurement at $\sqrt{s} = 350$ GeV. As an example, a model independent Higgs width Γ_H can be extracted with a precision of 5.0% using only the measurements performed at $\sqrt{s} = 350$ GeV. This precision can be further improved to 3.4% when combining the information from all studied CLIC energy stages assuming -80% electron beam polarisation for $\sqrt{s} = 1.4$ TeV and 3 TeV.

Table 3: The precisions of the Higgs observables at CLIC extracted using a model independent global fit based on the precisions listed in table 2 [5, 18] assuming -80% electron polarisation at $\sqrt{s} = 1.4$ TeV and 3 TeV.

Parameter	Measurement precision		
	350 GeV 500 fb^{-1}	+1.4 TeV +1.5 ab^{-1}	+3.0 TeV +2.0 ab^{-1}
m_H	120 MeV	30 MeV	20 MeV
λ	–	24%	11%
Γ_H [%]	5.0	3.6	3.4
g_{HZZ} [%]	0.8	0.8	0.8
g_{HWW} [%]	1.8	0.9	0.9
g_{Hbb} [%]	2.0	1.0	0.9
g_{Hcc} [%]	3.2	1.4	1.1
g_{Htt} [%]	—	4.1	4.1
$g_{H\tau\tau}$ [%]	3.5	1.6	< 1.5
$g_{H\mu\mu}$ [%]	—	14	5.6
g_{Hgg} [%]	3.6	1.1	1.0
$g_{H\gamma\gamma}$ [%]	—	5.7	< 5.7

Table 4: The precisions of the Higgs observables at CLIC extracted using a model dependent global fit with nine free parameters based on the precisions listed in table 2 [5, 18] assuming -80% electron polarisation at $\sqrt{s} = 1.4$ TeV and 3 TeV.

Parameter	Measurement precision		
	350 GeV 500 fb^{-1}	+1.4 TeV +1.5 ab^{-1}	+3.0 TeV +2.0 ab^{-1}
$\Gamma_{H,model}$ [%]	1.6	0.29	0.22
κ_{HZZ} [%]	0.43	0.31	0.23
κ_{HWW} [%]	1.5	0.15	0.11
κ_{Hbb} [%]	1.7	0.33	0.21
κ_{Hcc} [%]	3.1	1.1	0.75
κ_{Htt} [%]	—	4.0	4.0
$\kappa_{H\tau\tau}$ [%]	3.4	1.3	< 1.3
$\kappa_{H\mu\mu}$ [%]	—	14	5.5
κ_{Hgg} [%]	3.6	0.76	0.54
$\kappa_{H\gamma\gamma}$ [%]	—	5.6	< 5.6

When performing the global fit using LHC-like constraints – for instance assuming that there are no invisible Higgs decays and a fixed total Higgs width – subpercent precision of $\Gamma_{H,model}$ and κ_i are achieved as listed in table 4. Here, the κ_i are defined as the square root of the ratio of a Higgs partial width and its SM expectation

$$\kappa_i = \sqrt{\frac{\Gamma_i}{\Gamma_{i,\mathrm{SM}}}} \quad (3)$$

and the model-dependent Higgs total width is given by

$$\Gamma_{H,model} = \sum_i \kappa_i^2 \cdot BR_{i,SM}, \quad (4)$$

where the $BR_{i,SM}$ are the SM branching ratios for the respective final states. However, these results depend strongly on the fit assumptions. As an example, the model dependent Higgs width extraction has an improved precision of 1.6% for the measurements at $\sqrt{s} = 350\,\text{GeV}$ and of 0.22% when using all CLIC energy stages.

4. Summary

We presented the physics potential in terms of Higgs precision measurements of CLIC operating at three different energy stages. Measurements at $\sqrt{s} = 350\,\text{GeV}$ allow for a precise determination of the absolute values of a large variety of Higgs boson couplings. The energy stages $\sqrt{s} = 1.4\,\text{TeV}$ and 3 TeV increase the precision on these Higgs observables, and moreover give access to rare Higgs processes and decay modes and enable to study the Higgs self-coupling. A combined fit to all measurements performed in simulation has been presented which allows for a model independent extraction of the Higgs couplings and Higgs total width on the percent level. Higgs physics at CLIC is an active area with ongoing work and follow-up publications are in preparation.

References

[1] M. Aicheler, P. Burrows, M. Draper, T. Garvey, P. Lebrun, K. Peach, N. Phinney, H. Schmickler, D. Schulte, N. Toge (eds.), A Multi-TeV Linear Collider Based on CLIC Technology doi:10.5170/CERN-2012-007.

[2] L. Linssen, A. Miyamoto, M. Stanitzki, H. Weerts (eds.), CLIC Conceptual Design Report: Physics and Detectors at CLIC arXiv:1202.5940.

[3] P. Lebrun, L. Linssen, A. Lucaci-Timoce, D. Schulte, F. Simon, S. Stapnes, N. Toge, H. Weerts, J. Wells (eds.), The CLIC Programme: Towards a Staged e^+e^- Linear Collider Exploring the Terascale: CLIC Conceptual Design Report arXiv:1209.2543.

[4] J. Marshall, M. Thomson, Higgs Mass and Cross-Section Measurements at a 500 GeV CLIC Machine, Operating at $\sqrt{s} = 350\,\text{GeV}$ and 500 GeV, LCD-Note-2012-015.

[5] H. Abramowicz, et al., Physics at the CLIC e^+e^--Linear Collider – Input to the Snowmass process 2013 arXiv:1307.5288.

[6] S. Agostinelli, et al., Geant4: A Simulation toolkit, Nucl. Instrum. Meth. A506 (2003) 250. doi:10.1016/S0168-9002(03)01368-8.

[7] J. Allison, et al., Geant4 developments and applications, IEEE Trans. Nucl. Sci. 53 (2006) 270. doi:10.1109/TNS.2006.869826.

[8] T. Behnke, et al., The International Linear Collider Technical Design Report - Volume 4: Detectors arXiv:1306.6329.

[9] G. Aad, et al., Observation of a new particle in the search for the Standard Model Higgs boson with the ATLAS detector at the LHC, Phys. Lett. B 716 (2012) 1. arXiv:1207.7214, doi:10.1016/j.physletb.2012.08.020.

[10] S. Chatrchyan, et al., Observation of a new boson at a mass of 125 GeV with the CMS experiment at the LHC, Phys. Lett. B 716 (2012) 30. arXiv:1207.7235, doi:10.1016/j.physletb.2012.08.021.

[11] M. Thomson, $H \to WW^*$ at $\sqrt{s} = 1.4\,\text{TeV}$ and $HZ \to Hq\bar{q}$ at $\sqrt{s} = 350\,\text{GeV}$, Talk at the Linear Collider Workshop 2013.

[12] C. Grefe, T. Lastovicka, J. Strube, Prospects for the Measurement of the Higgs Yukawa Couplings to b and c quarks, and muons at CLIC, Eur. Phys. J. C73 (2013) 2290. arXiv:1208.2890, doi:10.1140/epjc/s10052-013-2290-4.

[13] G. Milutinovic-Dumbelovic, et al., SM-like Higgs decay into two muons at 1.4 TeV CLIC, Poster at the International Conference on High Energy Physics 2014.

[14] C. Grefe, Detector Optimization Studies and Light Higgs Decay into Muons at CLIC, Ph.D. thesis, University of Bonn, Germany, CERN-THESIS-2012-344 (Sep 2013).

[15] C. Grefe, E. Sicking, Physics potential of the $\sigma_{e^+e^-} \to H\nu_e\bar{\nu}_e \times BR_{H\to Z\gamma}$ measurement at a 1.4 TeV Compact Linear Collider, CLICdp-Note-2014-003.

[16] A. Robson, Higgs production in ZZ fusion at $\sqrt{s} = 1.4\,\text{TeV}$, Talk at the Linear Collider Workshop 2013.

[17] S. Redford, P. Roloff, M. Vogel, Physics potential of the top Yukawa coupling measurement at a 1.4 TeV Compact Linear Collider using the CLIC SiD detector, CLICdp-Note-2014-001.

[18] F. Simon, M. Szalay, P. Roloff, Combined Fits of CLIC Higgs Results for the Snowmass Process, LCD-Note-2013-012.